# Photosensitized Electron Injection in Colloidal Semiconductors

### Jacques Moser and Michael Grätzel\*

Contribution from the Institut de Chimie Physique, Ecole Polytechnique Fédérale, CH-1015 Lausanne, Switzerland. Received March 23, 1984

Abstract: Photosensitized electron injection in semiconductor particles was studied by using aqueous eosin (EO)/colloidal TiO<sub>2</sub> as the model system. Adsorption of EO onto the surface of TiO<sub>2</sub> occurs quantitatively at pH <6 and leads to red-shifted absorption and emission spectra. Electron injection in the conduction band of the TiO2 particles takes place from the S1 state of adsorbed eosin and occurs with a rate constant of  $8.5 \times 10^8$  s<sup>-1</sup> and a quantum yield of 38% (pH 3). The quantum yield decreases at high eosin occupancy of the particles due to concentration quenching. Back-electron transfer occurs via a rapid intraparticle reaction between EO+...e<sub>CB</sub> pairs associated with the same TiO<sub>2</sub> host aggregate and via a slower process involving bulk diffusion. The rate constant for intraparticle recombination is  $2 \times 10^5$  s<sup>-1</sup>, i.e.,  $4 \times 10^3$  times slower than that for electron injection. This enables light-induced charge separation to be sustained on a colloidal TiO<sub>2</sub> particle for several microseconds, which is sufficient to trap the electron by a noble metal deposit. Implications for light energy conversion devices are discussed.

The photosensitization of electron transfer across the semiconductor solution interface plays a vital role in silver halide photography<sup>1</sup> and electrophotography.<sup>2</sup> Recently, it has also gained interest with regards to light energy conversion in photoelectrochemical cells.3 Effort in this area has concentrated on improving the visible light response of wide-band semiconductors such as ZnO and TiO<sub>2</sub>. Sensitization is achieved by adsorption of dye molecules at the semiconductor surface which, upon excitation, inject an electron into its conduction band. The first successful experiment of this type was described by Putzeiko and Terenin,<sup>4</sup> who found that the Dember effect of ZnO powder in visible light was sensitized by xanthene and cyanine dyes. Numerous investigations with ZnO have followed their original report, owing mainly to the successful application of this material in reprographic processes.<sup>5</sup> Sensitization processes investigated with TiO<sub>2</sub> comprise the reduction of O<sub>2</sub> by hydroquinone<sup>6</sup> and water cleavage<sup>7</sup> as well as hydrogen generation<sup>8</sup> by visible light. Phthalocyanines,<sup>6</sup> Ru(bpy)<sub>3</sub><sup>2+</sup>, and derivatives<sup>7,8a</sup> as well as a Ti<sup>4+</sup>-chelate with 8-hydroxyquinoline<sup>8b</sup> were employed as sen-

While much important knowledge has been gathered over the years on the overall performance of dye-sensitized semiconductor systems,9 more information about the details of the electron-injection process is urgently required. The rapid nature of these reactions requires application of fast kinetic techniques which in the case of solid electrodes or powders is very difficult. On the other hand, semiconductor particles of colloidal dimensions are sufficiently small to yield transparent solutions, allowing for direct analysis of interfacial charge-transfer processes by a laser photolysis technique. 10 So far, there are very few time-resolved studies of dye sensitization with colloidal semiconductors. Terenin and Akimov<sup>11</sup> allude to flash photolysis of AgI colloids in the presence of dyes. Kiwi<sup>12</sup> examined electron transfer from excited Ru-(bpy), 2+ to colloidal TiO2 at elevated temperature. Very recently, the erythrosine sensitization of colloidal TiO2 in acetonitrile has been studied by Kamat and Fox.<sup>13</sup>

The present study employs eosin Y

as a sensitizer to study electron injection in colloidal TiO<sub>2</sub> particles. Precise information is available on the ground- and excited-state properties of this dye as well as the absorption spectra of its monoreduced and monooxidized radical forms, facilitating identification of transient species formed during the photoreaction. Apart from the initial charge-transfer event, we explore the fate of the injected electron, in particular its back reaction with the cation radical of the sensitizer, and the competing trapping by noble metals deposited on the surface of the semiconductor particle.

#### **Experimental Section**

Materials. TiCl<sub>4</sub> (Fluka purissimum) was further purified by vacuum distillation (40 °C, ca. 25 torr) to yield a colorless liquid. Colloidal TiO<sub>2</sub> particles were prepared by hydrolysis of this material at 0 °C according to a procedure previously described. 14 The mean particle radius obtained from electron microscopy and quasi-elastic light scattering is 50-60 Å. Electrophoretic measurements give a point of zero \( \zeta \) potential of 4.7. At pH ≤4 and pH ≥9, the TiO<sub>2</sub> sol is stable over at least several days, no

(1) Bourdon, J. J. Phys. Chem. 1965, 69, 705. (2) (a) Inoue, E. In "Current Problems in Electrophotography"; Borg, W. E., Hauffe, K., Eds.; de Gruyter: Berlin, 1972; p 146 ff. (b) Meier, H. "Die 

(3) (a) Gerischer, H.; Michel-Beyerle, M. E.; Rebentrost, F.; Tributsch, H. Electrochim. Acta 1968, 13, 150. (b) Tributsch, H.; Gerischer, H. Ber. Bunsenges. Phys. Chem. 1969, 73, 251. (c) Gerischer, H.; Willig, F. Top. Curr. Chem. 1976, 61, 31. (d) Spitler, M.; Calvin, M. J. Chem. Phys. 1977, 67, 5193. (e) Takizawa, T.; Watanabe, T.; Honda, K. J. Phys. Chem. 1980, 44, 51. (f) Iwasaki, T.; Oda, S.; Sawada, T.; Honda, K. Photogr. Sci. Eng. 1981, 25, 6. (g) Jaeger, C. D.; Fan, F. R. F.; Bard, A. J. J. Am. Chem. Soc. 1980, 102, 2592. (h) Watanabe, T.; Fujishima, A.; Honda, K. In "Energy Resources through Photochemistry and Catalysis"; Grätzel, M., Ed.; Academic Press: New York 1983 Press: New York, 1983.

(4) Putzeiko, E. K.; Terenin, A. Zh. Fiz. Khim. 1949, 23, 676.

(5) (a) Hauffe, K. Photogr. Sci. Eng. 1976, 20, 125. (b) Danzmann, H. J.; Hauffe, K. Ber. Bunsenges. Phys. Chem. 1975, 79, 439. (c) Agfa-Gevaert French Patent 1 547 196, 1966. (d) Lee, W. M. British Patent 1 267 308, 1969. (e) Brändli, R.; Rys, P.; Zollinger, H.; Oswald, H. R.; Schweizer, F. Helv. Chim. Acta 1970, 53, 1133.

(6) Fan, F. R. F.; Bard, A. J. J. Am. Chem. Soc. 1979, 101, 6139.
(7) Borgarello, E.; Kiwi, J.; Pelizzetti, E.; Visca, M.; Grätzel, M. Nature (London) 1981, 284, 158. J. Am. Chem. Soc. 1981, 103, 6423.
(8) (a) Hashimoto, K.; Kawai, T.; Sakata, T. Nouv. J. Chim. 1983, 7, 249.
(b) Houlding, V. H.; Grätzel, M. J. Am. Chem. Soc. 1983, 105, 5695.
Shimidzu, T.; Lyoda, T.; Koide, Y.; Kanda, N. Nouv. J. Chim. 1983, 7, 21.
(9) (a) Memming, R. Philips Tech. Rev. 1978, 38, 160. (b) Rajeshwar, K. Sirgh, P. Dupon, I. Elespechim, Apr. 1972, 23, 111. (c) Carischer H.

K.; Singh, P., DuBow, J. Electrochim. Acta 1978, 23, 111. (c) Gerischer, H. Ber. Bunsenges. Phys. Chem. 1973, 77, 771.

(12) Kiwi, J. Chem. Phys. Lett. 1981, 83, 594

(13) Kamat, P. V.; Fox, M. A. Chem. Phys. Lett. 1983, 102, 379. (14) (a) Moser, J.; Grätzel, M. Helv. Chim. Acta 1982, 65, 1436. (b)

Moser, J.; Grätzel, M. J. Am. Chem. Soc. 1983, 105, 6547.

<sup>(10) (</sup>a) Grätzel, M. Acc. Chem. Res. 1981, 14, 376. (b) Duonghong, D.; Borgarello, E.; Grätzel, M. J. Am. Chem. Soc. 1981, 103, 4685. (c) Duonghong, D.; Ramsden, J.; Grätzel, M. J. Am. Chem. Soc. 1982, 104, 2977. (11) (a) Terenin, A.; Akimov, I. A. J. Phys. Chem. 1965, 69, 730. (b) Terenin, A.; Akimov, I. A. Z. Phys. Chem. 1961, 217, 307.

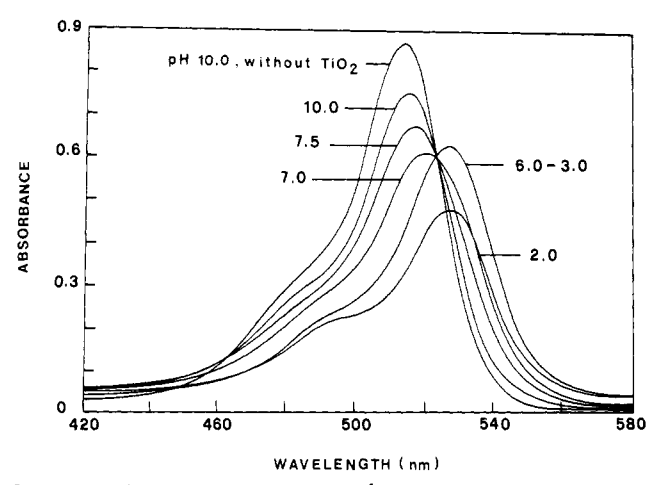


Figure 1. Absorption spectrum of  $10^{-5}$  M eosin solution in aqueous colloidal  $TiO_2$  (0.5 g/L) at different pH. Particles stabilized with PVA (1 g/L). Spectrum in PVA (1 g/L) solution at pH 10 is shown for comparison.

significant aggregation being detectable by a quasi-elastic light-scattering technique. In the intermediate pH domain the colloid requires a protective agent to prevent floculation. Poly(vinyl alcohol) was used in this case to stabilize the colloidal particles. Commercial PVA (Mowiol 98-10, Hoechst, West Germany) was treated by UV light to remove impurities.14 Control experiments showed that the protective agent had practically no effect on the characteristics of sensitized electron injection. Eosin Y, disodium salt (Fluka) was purified by column chromatography with use of neutral Al<sub>2</sub>O<sub>3</sub>. After it is eluted with a mixture of methanol/water/triethanolamine (90/9/1, v/v/v), the principal fraction is acidified with HCl and the precipitate is filtered and washed. protonated form of eosin is finally recrystallized from water until the product showed in alkaline solution an extinction coefficient for the absorption maximum at 516 nm of  $9.7 \times 10^4 \,\mathrm{M}^{-1} \,\mathrm{cm}^{-1}$ . Deionized water was distilled twice from a quartz still. All other products were at least reagent grade and used as supplied by the vendor.

Loading of the  ${\rm TiO_2}$  particles with Pt was carried out in the absence of stabilizer by photoplatinization.<sup>15</sup> A stock solution (volume 1.03 mL) containing  $2.5 \times 10^{-2}$  M  ${\rm H_2PtCl_6}$  was added to 100 mL of 5 g/L  ${\rm TiO_2}$  sol at pH 3, and after deaeration the solution was irradiated with a 450-W Xe lamp.  ${\rm H_2}$  appeared only after 48 h of light exposure. Irradiation was stopped at this time, and the solution was flushed with pure hydrogen gas to complete the reduction of  ${\rm PtCl_6}^{2-}$ . The calculated amount of Pt loading is 1% (w/w). The loading of  ${\rm TiO_2}$  with  ${\rm RuO_2}$  was carried out via decomposition of  ${\rm RuO_4}^{16}$  which occurs spontaneously according to eq  $1.^{17}$  The process is catalyzed by light. A volume of 0.38

$$RuO_4 \rightarrow RuO_2 + O_2$$
 (1)

mL of a  $5 \times 10^{-2}$  M aqueous stock solution of RuO<sub>4</sub> was added to 100 mL of unprotected TiO<sub>2</sub> sol (concentration 5 g/L, pH 3) and stirred in room light for 2 h. The calculated loading is 0.5% (w/w).

Apparatus. Laser photolysis experiments employed a Q-switched frequency-doubled ( $\lambda$  532 nm) Nd:YAG laser (JK 2000) combined with fast kinetic spectroscopy to detect transient species. <sup>18</sup> The pulse width was ca. 15 ns, and the energy delivered per pulse was 50 mJ. Fluorescence spectra were obtained with a Perkin-Elmer MPF 44 instrument and are corrected for the spectral response of the photomultiplier (Hamamatsu R 928) which is roughly flat in the range 400–800 nm. The samples were contained in a square quartz cuvette ( $10 \times 10$  mm), and the detector was always at 90° to the exciting light beam. UV-visible absorption spectra were recorded on a Cary 219 (Varian) spectrophotometer.

## Results and Discussion

85, 1850.

(i) Effect of Colloidal TiO<sub>2</sub> on the Absorption and Emission Characteristics of Eosin. The absorption spectrum of a  $10^{-5}$  M eosin solution in neutral or basic water shows a characteristic maximum at 516 nm with  $\epsilon = 9.7 \times 10^4$  M<sup>-1</sup> cm<sup>-1</sup> which arises

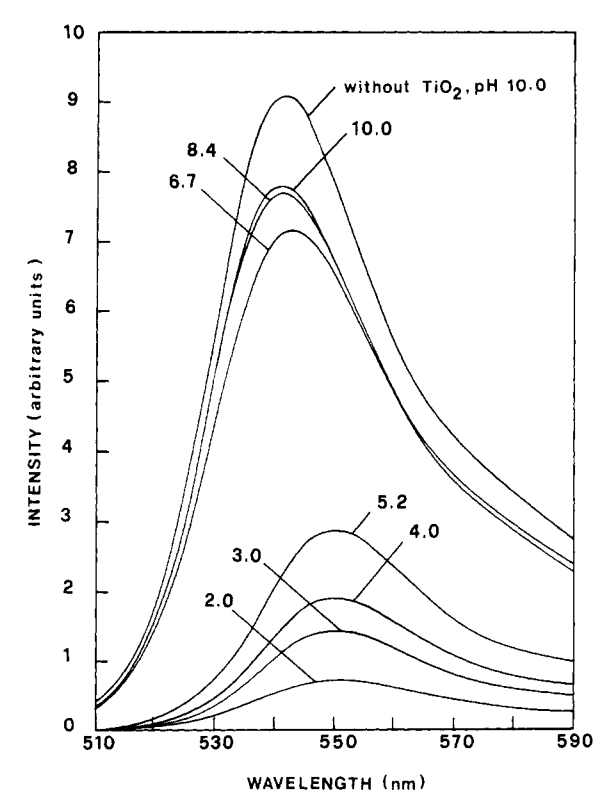


Figure 2. Effect of pH on the luminescence of eosin  $(10^{-5} \text{ M})$  in the presence of colloidal TiO<sub>2</sub> (0.5 g/L) protected by PVA (1 g/L).

from the dianionic form of the monomer dye. <sup>19</sup> Decreasing the pH below 5 shifts the absorption band to the red with  $\lambda_{max}$  520 nm at pH 3. We attribute this to the protonation of the phenolic hydroxyl group. Acid-base titration revealed the presence of one equivalent point, indicating pK<sub>1</sub>  $\simeq$  4.4.<sup>21</sup> The second pK could not be determined by this method since the neutral eosin molecule is insoluble in water.

Figure 1 shows the effect of pH on the eosin absorption in the presence of  $TiO_2$  (0.5 g/L). At pH 10 the spectrum is practically identical with that found in neutral or basic water. Decreasing the pH from 7.5 to 5 shifts the maximum to 527 nm. Associated with this transition is an isosbestic point at 523 nm. Within the pH range from 5 to 3 the spectral features remain essentially constant. The observed red shift in the absorption spectrum without notable change in its shape can be unambiguously attributed to the adsorption of monomer eosin dianion on the colloidal TiO<sub>2</sub> particle.<sup>22</sup> Coulombic interaction with the TiO<sub>2</sub> surface appears to play an important role since the spectral transition in Figure 1 occurs in a pH domain where the charge of the colloid changes from negative to positive. Quantitative determination of the adsorbed amount of eosin was carried out with 20 mL of buffered solution containing colloidal TiO<sub>2</sub> (2.5 g/L),  $5 \times 10^{-5}$  M eosin, and PVA stabilizer (5 g/L). The solution is enclosed in a dialysis membrane (cellulose acetate, pore diameter 15-30 Å) and stirred in 80 mL of buffered aqueous ambiant. Equilibrium was reached after ca. 40 h, and the concentration of free eosin was determined spectrophotometrically. From this procedure we find for the adsorbed fraction of eosin at pH 10, 7.2, and 4 the values 0.08, 0.52, and 0.95, respectively. This confirms the assignment of the spectra obtained for pH ≤5 in

<sup>(15)</sup> Kraeutler, B.; Bard, A. J. J. Am. Chem. Soc. 1978, 100, 4318.

<sup>(16)</sup> Humphry-Baker, R.; Lilie, J.; Grätzel, M. J. Am. Chem. Soc. 1982,

<sup>(17)</sup> The decomposition of RuO<sub>4</sub> can be followed spectrophotometrically, c.f.: Connick, R. E.; Hurley, C. R. J. Am. Chem. Soc. 1952, 74, 5012. (18) Rothenberger, G.; Infelta, P. P.; Grätzel, M. J. Phys. Chem. 1981,

<sup>(19)</sup> Eosin Y has only a weak tendency to form dimeric aggregates in aqueous solution (dimerization equilibrium constant 9  $\times$  10<sup>-3</sup>). Spectral evidence for dimer formation<sup>20</sup> ( $\lambda_{\rm max}$  531 and 487 nm,  $\epsilon_{\rm max}$  40 500 and 51 000 M<sup>-1</sup> cm<sup>-1</sup>) was found only at dye concentrations exceeding 5  $\times$  10<sup>-5</sup> M.

<sup>(20)</sup> Rohatapi, K. K.; Mukhophadhyali, A. K. Photochem. Photobiol. 1971, 14, 551.

<sup>(21)</sup> From spectral analysis we estimate for the protonation of the carboxyl group  $pK_2 \sim 3.4$ .

<sup>(22)</sup> Adsorption of eosin onto ZnO powder results in a similar shift of the dianion spectrum as observed here with colloidal TiO<sub>2</sub>; Iwasaki, T.; Oda, S.; Sawada, T.; Honda, K. J. Phys. Chem. 1980, 84, 2800.

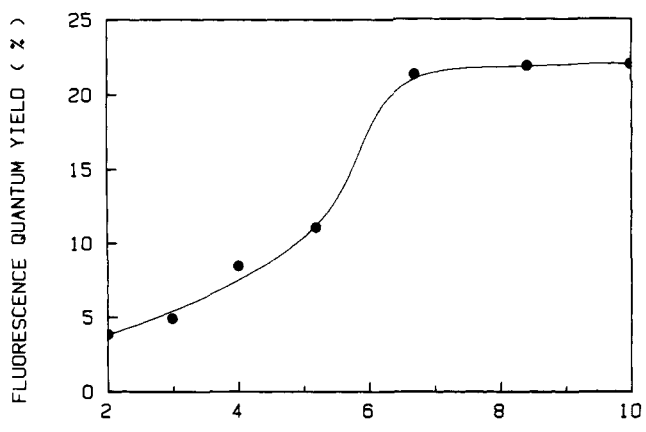


Figure 3. Effect of pH on the luminescence quantum yield of eosin in the presence of  $TiO_2$  (500 mg/L);  $\phi_F$  values obtained from integration of the emission curves in Figure 2. The quantum yield in pure water  $\phi_F$  = 0.22 was taken from Soep et al.<sup>27</sup>

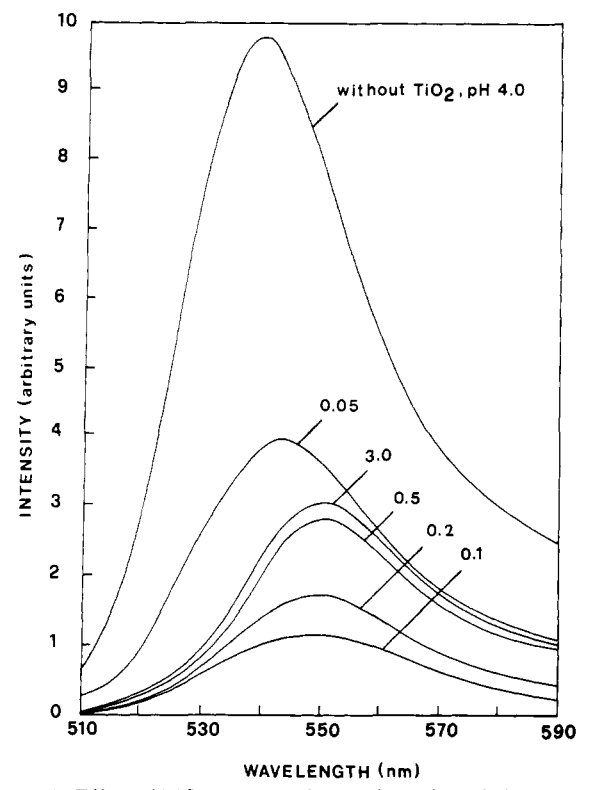


Figure 4. Effect of  $TiO_2$  concentration on the eosin emission spectrum at pH 4, dye concentration  $10^{-5}$  M. Practically identical results were obtained for unprotected and PVA-protected  $TiO_2$  solutions.

Figure 1 to the eosin associated with the surface of TiO<sub>2</sub> particles. Figure 2 illustrates the effect of pH on the luminescence of eosin in the presence of colloidal TiO2 (500 mg/L). At pH 10 the emission maximum is located at 540 nm and is identical with that found in water. Decreasing the pH from 7 to 5.2 leads to an abrupt red shift in the emission and marked reduction in its intensity. Below pH 5.2 the maximum in the luminescence remains at 550 nm while the intensity is further decreased. Figure 3 compares fluorescence quantum yields at the excitation wavelength ( $\lambda$  500 nm) for aqueous eosin solution of different pH in the presence of TiO<sub>2</sub> (500 mg/L). The quantum yield for the TiO<sub>2</sub> solution drops sharply between pH 6 and 4, i.e., in a pH domain where the transition from the free to the surface-bound state of the eosin dianion occurs. Since in TiO2-free solution the fluorescence changes very little between pH 7 and 4, one infers from these results that the luminescence of eosin is strongly quenched by the TiO<sub>2</sub> particles.

In Figures 4 and 5 the pH of the aqueous solution was maintained at 4 and the effect of colloidal TiO<sub>2</sub> on the eosin lu-

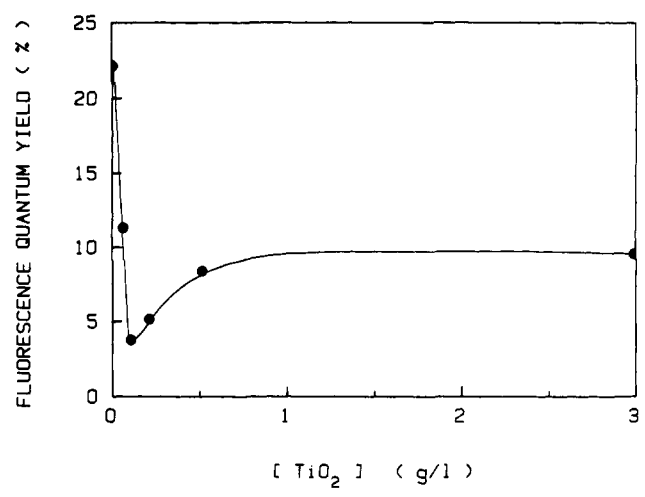


Figure 5. Effect of TiO<sub>2</sub> concentration on the fluorescence quantum yield of eosin calculated from the emission curves in Figure 4.

**Table I.** Concentration of  $TiO_2$  Particles and Average Occupancy of the Particles by Eosin at  $10^{-5}$  M Dye Concentration as a Function of Total  $TiO_2$  Concentration

[TiO <sub>2</sub> ], g/L	[particles], mol L <sup>-1</sup>	av no. of eosin molecules per particle
0.1	6.3 × 10 <sup>-8</sup>	160
0.2	$1.3 \times 10^{-7}$	80
0.5	$3.1 \times 10^{-7}$	32
1.0	$6.3 \times 10^{-7}$	16
3.0	$1.9 \times 10^{-6}$	5

minescence was investigated. Addition of TiO<sub>2</sub> (50 mg/L) leads to a pronounced decrease in the luminescence yield  $(\phi_f)$  and to a red shift in the emission maximum  $(\lambda_{max})$ . With 100 mg/L of TiO<sub>2</sub> present,  $\phi_f$  has dropped to 14% of its initial value and  $\lambda_{max}$  is ca. 548 nm. At this TiO<sub>2</sub> concentration  $\phi_f$  passes through a minimum. Further increase in TiO<sub>2</sub> concentration enhances the luminescence which at [TiO<sub>2</sub>]  $\geq$  0.5 g/L reaches a plateau corresponding to 32% of its intensity in pure water. No changes in  $\lambda_{max}$  occur in this concentration domain.

Since at a TiO<sub>2</sub> concentration of 100 mg/L eosin is quantitatively associated with the colloidal particles, the emission with  $\lambda_{max}$  548 nm can be attributed to the adsorbed state of the dye. Red shifts in the emission of xanthene dyes upon adsorption to metal oxide surfaces have been previously observed<sup>19</sup> and are due to hydrogen bond formation with surface hydroxyl groups. The displacement of the maximum is related to the polarizability and electronegativity of the metal cation. Thus, for fluorescein adsorbed onto Zn(OH)<sub>2</sub> and AlOOH,  $\Delta\lambda_{max}$  is 150 and 30 nm, respectively.<sup>23</sup> The relatively small red shift observed here for eosin indicates binding to OH groups at the TiO<sub>2</sub> surface with relatively acidic character.

In order to rationalize the drastic reduction in the eosin luminescence intensity upon adsorption to the  $TiO_2$  particles observed in Figures 4 and 5, we consider first concentration quenching. Deactivation via such a mechanism is suggested by the observation in Table I that the smallest emission intensity is obtained for the highest mean occupancy of the  $TiO_2$  particles by eosin, i.e., 160 molecules/particle. Under these conditions the surface concentration of eosin is  $2.1 \times 10^{13}$  cm<sup>-2</sup> and the mean distance between adjacent dye molecules is 22 Å. We expect in this case efficient dipolar energy transfer between adjacent eosin molecules until trapping by a molecular configuration favorable for radiationless deactivation quenches the excited state.<sup>24</sup> Concentration quenching was also encountered by Liang et al. in very recent

<sup>(23)</sup> Lendvay, E. J. Phys. Chem. 1965, 69, 738.

<sup>(24)</sup> We shall publish a detailed treatment of concentration quenching involving eosin adsorbed onto colloidal TiO<sub>2</sub> particles elsewhere. (Rothenberger, G.; Humphry-Baker, R.; Moser, J.; Grätzel, M., manuscript in preparation.)

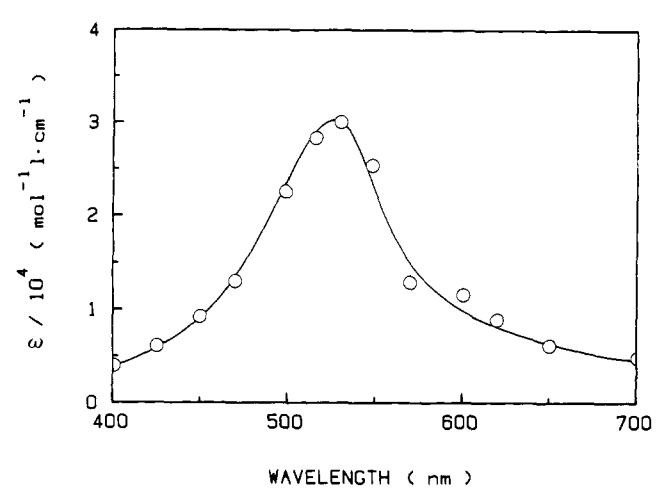


Figure 6. End-of-pulse spectrum obtained from the laser photolysis of 10<sup>-6</sup> M eosin in water, pH 10. The spectrum is corrected for ground-state bleaching. Extinction coefficients for the triplet state were obtained by using the method of Lachish et al. (Lachish, U.; Infelta, P. P.; Grätzel, M. Chem. Phys. Lett. 1979, 62, 317.)

picosecond time-resolved experiments with eosin monolayers adsorbed on tin oxide glass. The fluorescence lifetime  $\tau_f$  decreased from 1.4 ns in dilute aqueous solution to ca. 60 ps in the adsorbed state. These authors concluded that the reduction was due only to concentration quenching and not electron injection from the excited dye in the semiconductor. Consistent with the deactivation of excited eosin via concentration quenching is the observation in Figure 5 that the emission quantum yield passes through a minimum at 100 mg of TiO<sub>2</sub>/L, i.e., under conditions where the occupancy of TiO<sub>2</sub> particles by eosin is highest. Increasing the TiO<sub>2</sub> concentration decreases the particle occupancy by eosin (Table I), and this should diminish the efficiency of concentration quenching and hence increase  $\phi_f$  as is observed experimentally. However, Figure 5 shows also that decreasing the average occupancy below 32 eosin/particle does not lead to any further increase in the luminescence intensity which, at high TiO<sub>2</sub> concentration, remains 3 times lower than in TiO2-free solution. Since concentration quenching does no longer appear to play a significant role under these conditions, a second pathway for excited-state deactivation must prevail. This is investigated in the following by applying a laser photolysis technique.

(ii) Laser Photolysis Studies of Sensitized Electron Injection: Effect of pH and TiO<sub>2</sub> Concentration. Laser photolysis of eosin was first performed in pure water (pH 4) in the absence of TiO<sub>2</sub>. Transients were identified on the basis of earlier flash photolysis studies and literature absorption data for pertinent intermediates. The end of the pulse spectrum is identical with that of the triplet state  $(EO(T_1))$  which in aqueous solution is formed with a quantum yield of 0.76,26,27 Figure 6. In dearated solution the triplet decay obeys mixed first-/second-order kinetics. It is monitored at 600 nm where there is little interference from the absorption of ground-state eosin or ionic products formed during the triplet reaction. From the kinetic analysis, we obtain for the first half-lifetime 95 µs. Concomitantly with the triplet decay occurs the formation of eosin cation radicals (EO+) monitored at 450 nm. The EO<sup>+</sup> concentration attains a maximum after ca. 200 µs and decreases subsequently according to a second-order rate law. Associated with this decay is the recovery of  $EO(S_0)$ ground-state absorption recorded at 530 nm.

In accordance with earlier propositions, 27-29 we explain this

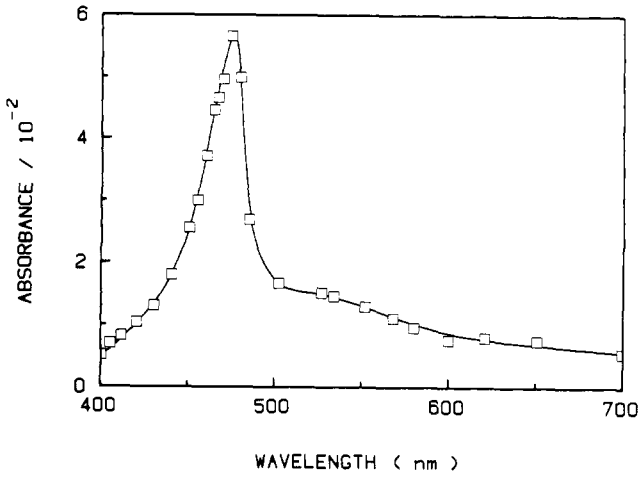


Figure 7. Transient spectrum obtained from the laser photolysis of 10<sup>-5</sup> M eosin in aqueous colloidal TiO<sub>2</sub> (pH 4) calculated from the absorbance change during the laser pulse and corrected for ground-state bleaching.  $[TiO_2] = 0.5 \text{ g/L}$ . Identical results were obtained for unprotected and PVA-protected solutions.

behavior with the following scheme (literature rate constants are given below the respective equation)

$$EO(S_0) \xrightarrow{h\nu} EO(S_1) \xrightarrow{\phi = 0.76} EO(T_0)$$
 (2)

$$EO(T_1) \to EO(S_0) \tag{3}$$

$$EO(T_1) + EO(S_0) \rightarrow 2EO(S_0)$$
 (4a)

$$3 \times 10^8 \text{ M}^{-1} \text{ s}^{-128}$$

$$EO(T_1) + EO(S_0) \rightarrow EO^+ + EO^-$$
 (4b)

$$7 \times 10^7 \,\mathrm{M}^{-1} \,\mathrm{s}^{-1.28}$$

$$2EO(T_1) \rightarrow 2EO(S_0)$$
 (5a)

$$2EO(T_1) \rightarrow EO^+ + EO^- \tag{5b}$$

eq 5a and 5b:  $1.3 \times 10^9 \text{ M}^{-1} \text{ s}^{-1.28}$ 

$$EO^{+} + EO^{-} \rightarrow 2EO(S_0) \tag{6}$$

$$8.8 \times 10^7 \text{ M}^{-1} \text{ s}^{-1.29}$$

The rate constants determined in our study are in agreement with the literature results apart from the value of  $k_6$  for which we find  $5 \times 10^9 \,\mathrm{M}^{-1} \,\mathrm{s}^{-1}$ . We confirm also that the formation of eosin cation radicals arises from the disproportionation of triplet states. (The concomitant formation of EO- could not be monitored since at pH 4 EO is protonated, pK 6.5.29) From the one-electron oxidation and reduction potentials of ground-state eosin, Eo- $(EO/EO^{+}) = 1.1 \text{ V}^{30} \text{ and } E^{\circ}(EO/EO^{-}) = 0.8 \text{ V (NHE)},^{31} \text{ and}$  the triplet-state energy of 1.98 eV<sup>30</sup>, the driving force for reaction 6 is only ca. 0.1 eV. The contribution of this process to EO+ formation is therefore small compared to that of reaction 5b.

Addition of colloidal TiO<sub>2</sub> introduces striking changes in the photoredox behavior of eosin. The transient spectrum obtained immediately after laser excitation of a deaerated 10<sup>-5</sup> M eosin solution in water (pH 4) containing colloidal TiO<sub>2</sub> (500 mg/L) is shown in Figure 7. It is distinguished by a prominent peak at 475 nm, a much weaker and broad absorption above 500 nm, and a shoulder at 400 nm. The spectrum is corrected for ground-state absorption within the wavelength region 440 nm ≤  $\lambda \leq 570$  nm. In Figure 7 the intense absorption with  $\lambda_{max}$  475 nm can be unambiguously attributed to the semioxidized eosin, EO<sup>+</sup>. Spectral characteristics are identical with those observed

<sup>(25)</sup> Liang, Y.; Goncalves, A. M.; Negus, D. K. J. Phys. Chem. 1983, 87,

<sup>(26)</sup> Fleming, G. R.; Knight, A. W. E.; Morris, J. M.; Robinson, G. W.;
Morrison, R. J. S. J. Am. Chem. Soc. 1977, 99, 4306.
(27) Soep, B.; Kellmann, A.; Martin, M.; Lindquist, L. Chem. Phys. Lett. 1972, 13, 241.

<sup>(28)</sup> Kasche, V.; Lindquist, L. Photochem. Photobiol. 1965, 4, 923

<sup>(29)</sup> Ohno, T.; Kato, S.; Koizumi, M. Bull. Chem. Soc. Jpn. 1966, 39, 232.

 <sup>(30)</sup> Loutfy, R. O.; Sharp, J. H. Photogr. Sci. Eng. 1976, 20, 165.
 (31) Literature values for E°(EO/EO<sup>-</sup>) are -0.85<sup>30</sup> and -0.79 V.<sup>32</sup>
 (32) Kepka, A. G.; Grossweiner, L. I. Photochem. Photobiol. 1971, 14,

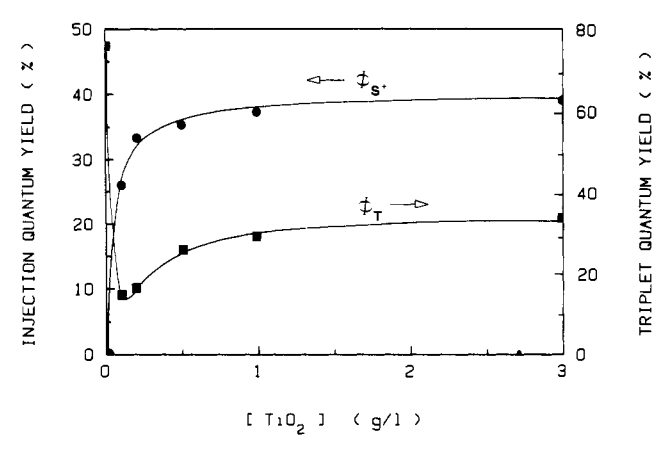


Figure 8. Effect of TiO<sub>2</sub> concentration on the quantum yield of eosin cation radical and triplet formation. Conditions as in Figure 7.

for EO<sup>+</sup> in water except that  $\lambda_{max}$  is red shifted by 13 nm.<sup>28</sup> A similar red shift, i.e., from 516 to 527 nm, occurred in the absorption maximum for  $EO(S_0)$  in Figure 1 upon adsorption onto the TiO<sub>2</sub> particles and was attributed to hydrogen bond formation with surface hydroxyl groups. That EO+ is produced from photoexcitation of EO(S<sub>0</sub>) in colloidal TiO<sub>2</sub> solution was recently confirmed by Rossetti and Brus33 using time-resolved laser Raman spectroscopy. The Raman spectrum of EO<sup>+</sup> associated with TiO<sub>2</sub> particles was different from that in pure water, and this was attributed to protonation of EO<sup>+</sup> by surface hydroxyl groups. The effect of TiO<sub>2</sub> concentration on the quantum yield of EO<sup>+</sup> formation,  $\phi[EO^+] = [EO^+]/[EO(S_0)]$ , where  $[EO(S_0)]$  is the concentration of eosin excited by the laser pulse, is illustrated in Figure 8. Concentrations of EO+ were calculated from the increase in 450-nm absorbance during the laser pulse by using  $\epsilon_{450}$  (EO<sup>+</sup>) 2.5 × 10<sup>-4</sup> M<sup>-1</sup> cm<sup>-1</sup>.<sup>34</sup> The concentration of EO(S<sub>1</sub>) was derived from the bleaching of ground-state absorption at 530 nm. 35 Quantum yield for EO<sup>+</sup> formation increases from 27% to 35% upon increasing the TiO2 concentration from 0.1 to 0.5 g/L and reaches a plateau value of 38% at 3 g/L of TiO<sub>2</sub>.

In Figure 7 the broad absorption at 600 nm and the shoulder at 400 nm arise from eosin triplet state<sup>25,27,37</sup> formed simultaneously with EO<sup>+</sup>. The quantum yield for triplet formation is also affected by the TiO2 concentration, and these results are included in Figure 8. These values were determined from the increase in 600-nm absorbance during the laser flash by using  $\epsilon_{600}(EO(T_1))$  $1.2 \times 10^4 \,\mathrm{M}^{-1} \,\mathrm{cm}^{-1}$ ;  $^{36} \,\phi_{\mathrm{T}} = 0.76$  for pure water was adopted from Soep et al.  $^{27}$  Upon addition of TiO<sub>2</sub> to an aqueous eosin solution of pH 4 the triplet yield declines sharply, attaining a minimum at 100 mg of TiO<sub>2</sub>/L. Further increase in colloid concentration leads to partial inversion of this effect:  $\phi_T$  augments until at  $[TiO_2]$  $\geq$  1 g/L a plateau value is reached where the triplet yield is 35%.

The effect of pH on both  $\phi_T$  and  $\phi(EO^+)$  at a fixed TiO<sub>2</sub> concentration of 500 mg/L is illustrated in Figure 9. Above pH 6 the triplet yield is essentially the same as in pure water. It declines sharply between pH 6 and 5 and more gradually at lower pH. The inverse trend is observed for the efficiency of EO<sup>+</sup>

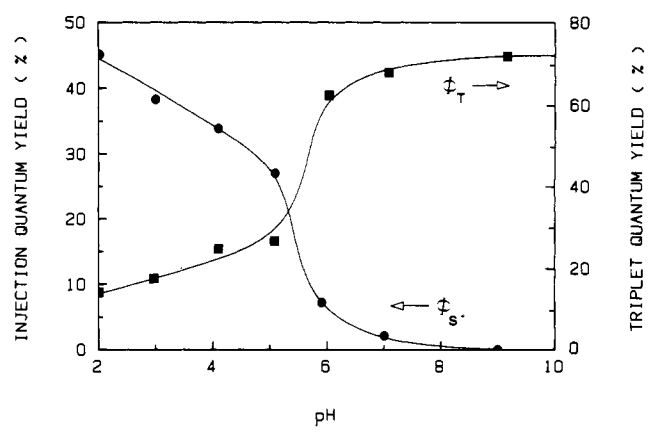


Figure 9. Effect of pH on the quantum yield of eosin cation radical and triplet formation at a fixed concentration of colloidal TiO2 of 500 mg/L, [PVA] = 1 g/L.

formation, which is very small in neutral solution and increases steeply upon decreasing the pH below 6.

It was shown above that in pure water the photogeneration of EO+ is a relatively slow and inefficient process, arising from the dismutation of eosin triplet states. By contrast, in the presence of colloidal TiO<sub>2</sub>, EO<sup>+</sup> is generated efficiently and at a high rate, its formation being completed within the 15-ns duration of the laser pulse. In this case the mechanism of EO+ formation is different from that in water and involves electron injection from the electronically excited eosin into the conduction band of the colloidal TiO<sub>2</sub> particle. Furthermore, we can identify the S<sub>1</sub> state of the dye as the active intermediate in the charge-transfer process,

$$EO(S_1) \xrightarrow{k_{inj}} EO^+ + e_{CB}^-(TiO_2)$$
 (7)

The thermodynamic driving force for reaction 7 is given by the difference between the redox potential of  $EO(S_1)$  and the conduction band position of colloidal TiO2, ECB. For the former a value of -1.2 V (NHE) is derived from the ground-state potential and the singlet excitation energy of  $2.3 \text{ eV}^{30}$  while the latter has been experimentally determined as  $^{10c}E_{CB} = -0.1 - 0.059 \text{ pH}$ . Thus, there is sufficient driving force for reaction 7 even under alkaline conditions. Nevertheless, charge injection is only observed at pH ≤6, i.e., under conditions where eosin is associated with the TiO<sub>2</sub> particles. This is reasonable since close proximity of the reactants is required for electron transfer to compete with the two other channels of singlet deactivation, i.e., intersystem crossing as well as radiative and nonradiative deactivation:

$$EO(S_1) \xrightarrow{k_{isc}} EO(T_1)$$
 (8)

$$EO(S_1) \xrightarrow{k_\tau} EO(S_0) + h\nu \tag{9a}$$

$$EO(S_2) \xrightarrow{k_{rr}} EO(S_0)$$
 (9b)

The formation of EO<sup>+</sup> during the photolysis of eosin/TiO<sub>2</sub> solutions could arise from reactions other than (7). One possibility is electron transfer from the triplet state into the conduction band of the TiO<sub>2</sub> particles:

$$EO(T_1) \rightarrow EO^+ + e_{CB}^- \tag{10}$$

The driving force for reaction 10, derived from the standard potential of the EO( $T_1$ )/EO<sup>+</sup> couple,  $E^{\circ} = -0.9 \text{ V (NHE)}$ , is ca. 0.5 eV at pH 5, increasing further by 59 mV with each decreasing pH unit. In spite of these favorable thermodynamic conditions, charge injection from the triplet does not occur: The triplet lifetime for eosin associated with colloidal TiO2 is the same as that in pure water, i.e., between 100 and 200  $\mu$ s. This shows that any electron transfer via reaction 10 must be much slower than the other triplet deactivation processes.

A second possibility is the generation of EO<sup>+</sup> via triplet-ground state or triplet-triplet dismutation, reactions 4b and 5b. While

<sup>(33)</sup> Rossetti, R.; Brus, L. E. J. Am. Chem. Soc., in print. We thank Dr. L. Brus for communcating to us these results prior to publication.

<sup>(34)</sup> The absorption maximum of EO<sup>+</sup> adsorbed onto TiO<sub>2</sub> is at 475 nm and hence red shifted by 13 nm with respect to  $\lambda_{max}$  in water.<sup>28</sup> In the calculation of EO<sup>+</sup> concentration, we assume that the extinction coefficient at the maximum ( $\epsilon = 6 \times 10^4 \,\mathrm{M}^{-1} \,\mathrm{cm}^{-1}$ ) is not affected by the adsorption.

<sup>(35)</sup> The signal at 530 nm contains a negative contribution from EO(S<sub>0</sub>) bleaching and a positive one from EO( $T_{1}$ ):  $\Delta A_{530} = -\epsilon_{EO(S_{0})}[EO(S_{0})] + \epsilon_{EO(T_{1})}[EO(T_{1})]$ . Extinction coefficients used in the calculation are  $\epsilon_{EO(S_{0})} = 6 \times 10^{4} \text{ M}^{-1} \text{ cm}^{-1}$  and  $\epsilon_{EO(T_{1})} = 3.0 \times 10^{4} \text{ M}^{-1} \text{ cm}^{-1}$ . The concentration of triplet states was independently determined from the transient absorbance at 600 nm. Due to a relatively large uncertainty in the extinction coefficients for the triplet state at 530 and 600 nm, the error limit of the  $\phi(EO+)$  values

<sup>(36)</sup> This value was determined by us from aqueous eosin solution without TiO<sub>2</sub>. Literature values for  $\epsilon_{500}(\text{EO}(T_1))$  are  $1.5 \times 10^4 \, \text{M}^{-1} \, \text{cm}^{-1.32}$  and  $7 \times 10^3 \, \text{M}^{-1} \, \text{cm}^{-1.28}$  Bowers and Porter report  $\epsilon_{518} = 2.8 \times 10^4 \, \text{M}^{-1} \, \text{cm}^{-1.37}$  (37) Bowers, P. G.; Porter, G. *Proc. R. Soc. London, Ser. A* 1967, A297,

these processes are comparatively slow in pure water, they could be accelerated significantly when they occur on a TiO<sub>2</sub> particle. The kinetics of chemical reactions between species restricted in their diffusional motion to the surface of a spherical aggregate have been previously analyzed.<sup>38</sup> For a pair of eosin triplets associated with a 110 Å size TiO<sub>2</sub> particle, the average time between two encounters is 0.07 and 1.5 µs depending on the diffusion coefficient of the reactants at the TiO<sub>2</sub> surface.<sup>39</sup> This is much longer than the EO+ formation time which was observed here to occur within the 10-ns laser pulse. Note also that  $\phi(EO^+)$ in Figure 9 increases with TiO<sub>2</sub> concentration, i.e., with decreasing eosin occupancy of the particles. The opposite trend would be expected if intraparticle triplet dismutation made a significant contribution to EO<sup>+</sup> formation. Furthermore,  $\phi(EO^+)$  remains at the maximum value of 38% at pH 4 even when only one eosin molecule is associated with a TiO<sub>2</sub> particle, i.e., under conditions where no intraparticle reactions are possible.

We thus conclude that the primary photochemical events in the  $\cos$ in/TiO<sub>2</sub> solutions are adequately described by eq 7–9. The relative contributions of these three reactions to the deactivation of EO(S<sub>1</sub>) depend strongly on both TiO<sub>2</sub> concentration and pH. In order to explain the TiO<sub>2</sub> concentration dependency of the parameters  $\phi_F$ ,  $\phi_{EO^+}$ , and  $\phi_T$ , we draw attention to the fact that the nonradiative decay constant, and hence  $\tau$ 

$$\tau = (k_{\rm nr} + k_{\rm r} + k_{\rm isc} + k_{\rm ini})^{-1} \tag{11}$$

are strongly influenced by the eosin occupancy of the particles. The closer the distance between adjacent dye molecules on the  $TiO_2$  surface, the more efficient will be the concentration quenching, i.e., the higher the value of  $k_{nr}$  will be and the smaller the luminescence lifetime  $\tau$ . We observe in Figure 5 a minimum for  $\phi_F$  at low  $TiO_2$  concentration when the particle occupancy is maximal. The same minimum is found for  $\phi_T$  in Figure 8 since both quantum yields are directly proportional to  $\tau$ , i.e.

$$\phi_{\rm F} = k_{\rm r} \tau \tag{12}$$

$$\phi_{\rm T} = k_{\rm isc} \tau \tag{13}$$

Increasing the  ${\rm TiO_2}$  concentration leads to a decrease in the average occupancy of the particles by eosin and hence in the value of  $k_{\rm nr}$ . As a consequence, the parameters  $\tau$ ,  $\phi_{\rm F}$ , and  $\phi_{\rm T}$  increase and attain a plateau at higher  ${\rm TiO_2}$  concentration where the influence of concentration quenching becomes negligible.

The effect of pH is to change the rate of charge injection apart from influencing the adsorption of eosin to the TiO<sub>2</sub> particles. Thus, in the pH domain from 5 to 2, practically all the eosin is associated with the TiO<sub>2</sub> colloid. Nevertheless the quantum yield of EO<sup>+</sup> formation increased from 27% to 45%. This is attributed to an increase in the charge injection rate constant

$$k_{\rm inj} = \phi_{\rm EO^+}/\tau \tag{14}$$

resulting from the augmentation of the driving force for reaction 7 which is 0.8 and 0.98 eV at pH 5 and 2, respectively. Apparently, in the photosensitized electron transfer from eosin to the conduction band of TiO<sub>2</sub>, a relatively large expenditure of free energy is required to obtain fast reaction rates. We have calculated the absolute value of  $k_{\rm inj}$  for 3 g/L TiO<sub>2</sub> solutions of pH 3 where  $\phi_{\rm F}=0.09$ ,  $\phi_{\rm T}=0.18$ , and  $\phi_{\rm inj}=0.4$ . Using eq. 11–14 one derives  $k_{\rm r}/k_{\rm nr}=0.27$ ,  $k_{\rm isc}/k_{\rm nr}=0.55$ , and  $k_{\rm inj}/k_{\rm nr}=1.21$ . Assuming that the radiative decay for eosin(S<sub>1</sub>) adsorbed on TiO<sub>2</sub> occurs with the same rate as in ethanol, <sup>26</sup>  $k_{\rm r}=1.91\times10^8~{\rm s}^{-1}$  (the emission spectrum of EO(S<sub>1</sub>) in ethanol has the same shape and  $\lambda_{\rm max}$  as in colloidal TiO<sub>2</sub> solution), one obtains

$$k_{\rm ini}(pH\ 3) = 8.5 \times 10^8\ s^{-1}$$

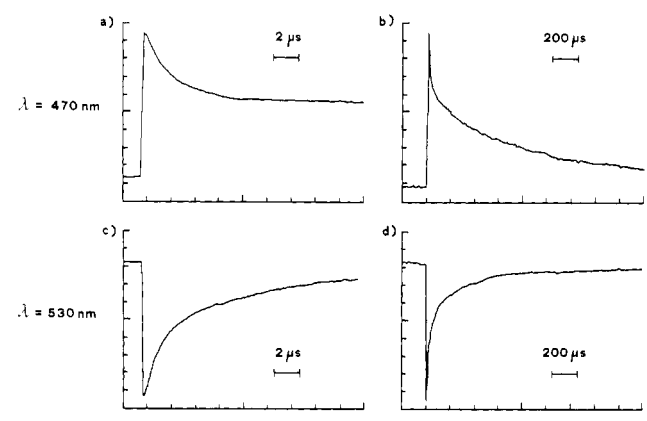


Figure 10. Oscillograms from the laser photolysis of  $10^{-5}$  M eosin in aqueous colloidal TiO<sub>2</sub> (3 g/L), pH 3; no protective polymer was used. The temporal characteristics of the EO<sup>+</sup> decay at 470 nm and the ground-state bleaching at 530 nm are displayed on two different time scales. Note that the eosin triplet absorbance makes a contribution to the 530-nm signal.

**Table II.** Average Number of Injected Electrons per TiO<sub>2</sub> Particle as a Function of TiO<sub>2</sub> Concentration for the Experimental Conditions Used in Figures 7-12

$[TiO_2], g/L$	$\bar{n}_{e}$ -(TiO <sub>2</sub> ) particle	
0.1	17.1	
0.2	10.2	
0.5	5.4	
1.0	3.0	
3.0	1.0	
3.0	1.0	

(iii) Intra- vs. Interparticle Back-Electron Transfer. In the following section we shall examine the fate of the electron injected into the conduction band of the TiO<sub>2</sub> particle. In particular, we are interested in the dynamics of interfacial back-electron transfer to the eosin parent cation. Figure 10 shows oscillograms from the laser photolysis of aqueous eosin solutions (pH 3) containing colloidal TiO<sub>2</sub> (3 g/L). The vertical rise in the 470-nm absorbance indicates formation of EO+ during the light pulse. The subsequent decay of the EO+ absorption is biphasic: a fast initial component which is completed within ca. 10  $\mu$ s (Figure 10a) is followed by a much slower decrease (Figure 10b) occurring over several hundred microseconds. The temporal behavior of the EO ground-state bleaching was also examined and was found to correspond to the mirror image of the EO<sup>+</sup> absorption decay in Figure 10c,d. Both the fast component of the EO<sup>+</sup> decay and the bleaching recovery of  $EO(S_0)$  obey first-order kinetics. From computer analysis of the oscilloscope traces in Figure 10 a rate constant of  $4 \times 10^5$  s<sup>-1</sup> is obtained. The subsequent slower EO<sup>+</sup> reaction was found to follow mixed first-/second-order kinetics, the initial half-lifetime being ca. 230  $\mu$ s. After completion of the EO<sup>+</sup> decay 96% of the eosin concentration that was transformed into cation radicals during the laser pulse is recovered. The remainder is irreversibly bleached.40

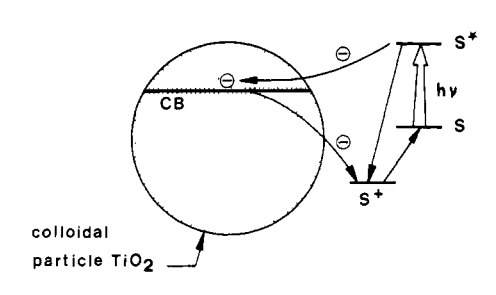
Note that the conditions in Figure 10 were selected such that at most one electron was injected into a  $TiO_2$  particle. The average number of injected charges per particle  $(n_e-(TiO_2))$  increases with decreasing  $TiO_2$  concentration, Table II. Under conditions where  $n_e-(TiO_2) > 1$  we observe also a biphasic behavior in the decay of  $EO^+$ . However, the kinetics of the fast step follow here a complex, presumably multiexponential time law. The fraction of  $EO^+$  decaying in this initial rapid process as well as its rate was found to increase with the number of electrons injected into a  $TiO_2$  particle.

In order to rationalize these observations, we use the scheme shown in Figure 11a. Excitation of eosin to the  $S_1$  state leads to injection of an electron into the  $TiO_2$  particle, leaving semi-

<sup>(38)</sup> Hatley, M. D.; Kozak, J. J.; Rothenberger, G.; Infelta, P. P.; Grätzel, M. J. Phys. Chem. 1980, 84, 1508.

<sup>(39)</sup> Detailed analysis is given in ref 38 for the case of reactions on the surface of micellar assemblies. Since eosin is linked to the TiO<sub>2</sub> particles through hydrogen bonds, its diffusional motion on the surface may be slower than that considered there.

<sup>(40)</sup> We attribute this irreversible bleaching to a side reaction of EO<sup>+</sup> which by analogy with fluorescein is probably dimerization, c.f.: Lindquist, L. J. Phys. Chem. 1963, 67, 1701.



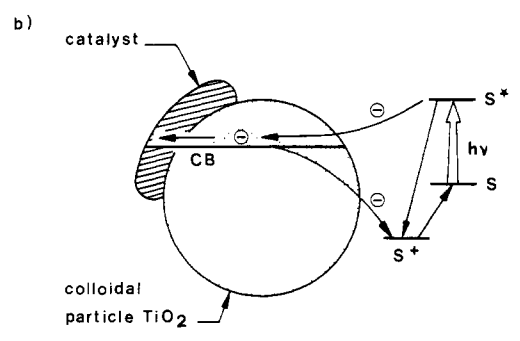


Figure 11. Schematic illustration of charge injection and intraparticle back-electron transfer in the photosensitization of a colloidal semiconductor particle: (a) without redox catalyst, (b) noble metal catalystloaded particle.

oxidized eosin behind on the surface. The subsequent backelectron transfer

$$e_{CB}^{-} + EO^{+} \rightarrow EO(S_{0})$$
 (15)

occurs in two steps.

The fast initial part involves e<sub>CB</sub>-...EO+ pairs associated with their original TiO<sub>2</sub> host particle. Such an intraparticle process is expected to obey first-order kinetics<sup>41-43</sup> if only one pair per particle participates in the reaction, as is the case under the experimental conditions employed in Figure 10. Only a fraction of 50% of the eosin cation radicals produced by the laser pulse undergoes this rapid back reaction. The remainder desorbs from the TiO<sub>2</sub> particle and escapes into the solution bulk. This part will undergo slow back reaction which involves diffusional encounter of EO<sup>+</sup> and TiO<sub>2</sub> particles (interparticle mechanism). For the rapidly decaying fraction of EO+, we can write

$$f(EO^+) = \frac{k_b}{k_b + k_d} = \frac{k_b}{k_{obsd}} = 0.5$$
 (16)

where  $k_b$  and  $k_d$  are the specific rates (in s<sup>-1</sup>) of intraparticle back reaction and desorption of EO<sup>+</sup> and  $k_{\rm obsd} = 4 \times 10^5 \, \rm s^{-1}$  is the observed rate constant for the fast EO<sup>+</sup> decay. From eq 16 we obtain

$$k_{\rm b} = 2 \times 10^5 \, {\rm s}^{-1}$$

corresponding to a mean lifetime of 5 µs for a e<sub>CB</sub>-...EO<sup>+</sup> pair associated with a TiO<sub>2</sub> particle. The intraparticle back reaction itself is composed of two elementary steps comprising diffusion of the injected charge to the particle surface and subsequent interfacial electron transfer to the EO+ parent ion. The rate parameter  $k_b$  can therefore be expressed as

$$k_{\rm b}^{-1} = k_{\rm diff}^{-1} + (k_{\rm ini}^{-})^{-1}$$
 (17)

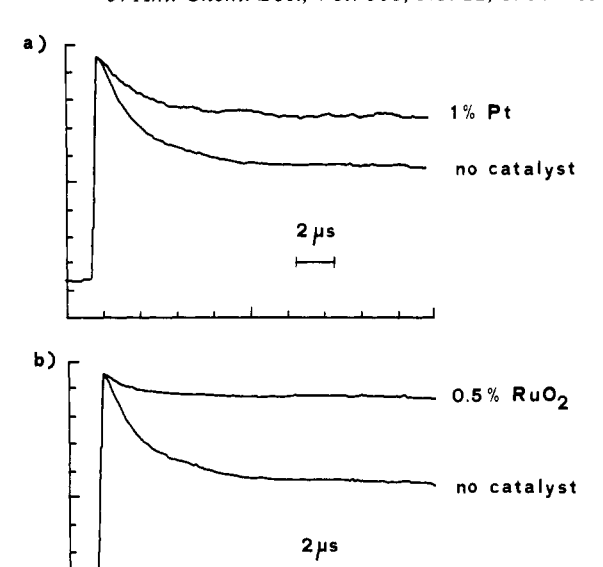


Figure 12. Oscillograms from the laser photolysis of 10<sup>-5</sup> M eosin in aqueous colloidal TiO<sub>2</sub> (3 g/L), pH 3, no protective polymer present. The effect of noble metal loading on the intraparticle electron transfer is investigated by monitoring the EO+ decay at 470 nm.

where  $k_{\text{diff}}$  and  $k_{\text{inj}}$  are the specific rates of these individual processes. Since

$$k_{\rm diff} \simeq \frac{1}{\tau_{\rm diff}} r_{\rm s} \tag{18}$$

where  $\tau_{\text{diff}} = 2.5$  ps is the average diffusion time for an electron from the particle interior to the surface<sup>44</sup> and  $r_s = 3.6 \times 10^{-3}$  is the area ratio of an eosin molecule and the surface of a TiO<sub>2</sub> particle, we can estimate for  $k_{\text{diff}}$  a value of 1.5 × 10<sup>9</sup> s<sup>-1</sup>. This is much bigger than the experimentally derived value for  $k_b$ . Therefore, in the back reaction of e<sub>CB</sub> with EO+, the electron transfer at the interface is rate determining,  $k_b \simeq k_{\rm inj}$ . Note that this reverse electron transfer occurs at ca.  $4 \times 10^3$  times smaller rate than the forward injection from the EO(S<sub>1</sub>) state into the TiO<sub>2</sub> particle. Such a behavior is in accordance with the predictions of classical electron-transfer theory.45 The highly exothermic nature of the back-electron transfer ( $\Delta G = -1.5 \text{ eV}$ ) is expected to result in a decrease in reaction rate. However, we draw attention to the fact that classical theory may not be applicable in the inverted region. Thus, reduction of aromatic cation radicals by conduction band electrons of ZnO electrodes is not significantly affected by the driving force and occurs very rapidly despite the highly exothermic character of these reactions.<sup>46</sup> (One referee pointed out that the entropy, i.e., phase space factor associated with the volume of the TiO2 particle, should make the back-transfer rate slow. Marcus theory does not incorporate this.)

The relatively slow rate of intraparticle back reaction between e<sub>CB</sub> and EO<sup>+</sup> is a desirable feature from the viewpoint of light energy conversion. It allows photoinduced charge separation to be sustained over a sufficiently long time so that a significant fraction of  $EO^+$  can escape from the  $TiO_2$  particles into the solution. Once in the aqueous bulk, EO+ will still undergo back reaction with e<sub>CB</sub><sup>-</sup>(TiO<sub>2</sub>). However, this involves bulk diffusion and hence occurs at a much slower rate than intraparticle back-electron transfer. Desorption of EO+ from the surface of TiO<sub>2</sub> is more easy than that of the eosin parent molecule due to decreased Coulombic attraction.

(iv) Photosensitized Electron Injection into Noble Metal Loaded TiO<sub>2</sub> Particles. In the following we report on some preliminary

<sup>(41)</sup> The situation is equivalent to the case of intramicellar electrontransfer kinetics which are dealt with in references 38, 42 and 43

<sup>(42)</sup> Maestri, M.; Infelta, P. P.; Grätzel, M. J. Chem. Phys. 1978, 69,

<sup>(43)</sup> Moroi, Y.; Infelta, P. P.; Grätzel, M. J. Am. Chem. Soc. 1979, 101,

<sup>(44)</sup> Grätzel, M.; Frank, A. J. J. Phys. Chem. 1982, 86, 2964.(45) Marcus, R. A. J. Chem. Phys. 1956, 24, 966; 1956, 24, 979; 1957,

<sup>(46)</sup> Nakabayashi, S.; Itoh, K.; Fujishima, A.; Honda, K. J. Phys. Chem. 1983, 87, 5301.

experiments designed to study the trapping of photoinjected electrons by catalysts deposited on the surface of the TiO<sub>2</sub> particles. Figure 12b shows oscilloscope traces obtained from the laser photolysis of eosin in colloidal TiO<sub>2</sub> loaded with 0.5% RuO<sub>2</sub>. The vertical rise of the absorbance signal at 470 nm indicates formation of EO+ during the light pulse. From this absorbance increase the quantum yield of charge injection was determined at 0.4 which is slightly higher than in the absence of RuO<sub>2</sub>. The features of the EO+ decay are strikingly different from that observed for bare TiO<sub>2</sub> particles in that there is no fast component characteristic for intraparticle electron transfer. The EO<sup>+</sup> absorption decays here in a smooth and relatively slow fashion with a first halflifetime of 240 µs. Kinetics of ground-state bleaching monitored at 530 nm correspond to the mirror image of the 470-nm absorbance decay.

Similar effects are observed when Pt instead of RuO2 is deposited onto the TiO<sub>2</sub> particles, Figure 12a. In this case, more catalyst is required to eliminate the fast step in the EO<sup>+</sup> reaction. Thus, at 1% Pt loading the initial rapid decline in the 470-nm signal is still perceptible and constitutes 25% of the total absorbance change induced by the laser pulse, as compared to 50% for Pt-free TiO<sub>2</sub> particles.

These observations are rationalized in terms of the scheme shown in Figure 11b. The role of the catalyst is to trap photoinjected electrons and to intercept in this way their back reaction with EO<sup>+</sup> adsorbed at the particle surface. This allows a larger fraction, or all of the EO+ formed during the laser pulse, to escape in solution. As was discussed above, the subsequent back reaction is relatively slow since it involves bulk diffusion. Also, the species that reduced EO+ is not e<sub>CB</sub>- but rather an H- atom adsorbed at the catalyst surface, or in the case of RuO<sub>2</sub> a ruthenium lattice ion with a <4+ valency.

From Figure 11a one can derive an absolute value for the rate constant of electron transfer from the conduction band of the TiO2 particle to the Pt deposit on the surface. At 1% loading the fraction of EO<sup>+</sup> participating in the fast decay is 0.25, and the observed rate constant for this rapid charge recombination process is  $6 \times 10^5$  s<sup>-1</sup>. By analogy with eq 16, we write

$$f(EO^+) = \frac{k_b}{k_{obsd}} = 0.25$$
 (19)

where

$$k_{\text{obsd}} = k_{\text{b}} + k_{\text{d}} + k_{\text{trap}} \tag{20}$$

One obtains therefore  $k_{\text{trap}} = 2.5 \times 10^5 \text{ s}^{-1}$ . A conspicuous feature of Figure 12 is that at comparable loading RuO<sub>2</sub> is more effective as a e<sub>CB</sub> scavenger than Pt. Trapping efficiencies are related to the dispersion of the catalyst and the nature of the junction formed at the semiconductor/metal interface. Ohmic contact is necessary for electron transfer to occur rapidly. However, from the work function of Pt ( $\phi = 5.2 \text{ eV}^{47}$ ) or RuO<sub>2</sub> ( $\phi = 4.8 \text{ eV}^{48}$ ) and the electron affinity of TiO<sub>2</sub> ( $\chi = 4.0 \text{ eV}^{49}$ ), one would predict that a rectifying barrier of 1.2 or 0.8 V, respectively, should be produced at the junction of TiO<sub>2</sub> with these catalysts. This would impair electron transfer from the conduction band of the particle to the noble metal deposit. However, Hope and Bard<sup>50</sup> have shown that the electrical contact between Pt and TiO<sub>2</sub> is often ohmic due to the interdiffusion of

the two materials. They also predict that due to the high density of surface states the junction between a colloidal TiO<sub>2</sub> particle and Pt should have a low resistance. This view is supported by the work of Aspnes and Heller,<sup>51</sup> who found that hydrogen adsorption on Pt decreases its work function, rendering its contact with TiO<sub>2</sub> ohmic. The eosin/TiO<sub>2</sub> system lends itself to an investigation of the effects of ambients such as H<sub>2</sub> on the rate of electron trapping by a noble metal deposit.<sup>52</sup> Such studies are expected to give clues as to the nature of the catalyst/TiO<sub>2</sub> junction when the particles are suspended in water and exposed to reducing or oxidizing atmospheres. These effects are presently being investigated further.

#### Conclusions

Using eosin/colloidal TiO<sub>2</sub> solutions as a model system, we have performed here a detailed study to scrutinize the salient features that control photosensitized electron injection from an excited dye in the conduction band of a semiconductor particle. Charge transfer occurs from the excited eosin singlet and competes with other radiative and nonradiative deactivation routes. Adsorption of eosin to the TiO<sub>2</sub> surface is a prerequisite for successful photosensitization. Low pH and high TiO<sub>2</sub> concentration favor charge injection. This is due to an increase in driving force of the reaction and dilution of the surface concentration of the dye, respectively. At high eosin occupancy of the particles, concentration quenching occurs, and we shall model this process using a statistical approach that takes into account the distribution of interacting species in the compartimentalized reaction space. Concentration quenching is likely to account for the low efficiency (2-3%) of the photocurrent generation in photoelectrochemical cells using eosin adsorbed on single crystal TiO2 electrodes. The advantage of colloidal semiconductor solutions demonstrated in this study is that the undesirable effect of concentration quenching can readily be eliminated and that the efficiency of charge injection is greatly increased by increasing the particle concentration.

An important aspect of this work concerns the fate of the electron photoinjected in the colloidal semiconductor particle, in particular its back reaction with the parent cation. For the first time it has been possible to monitor directly the kinetics of this process. A first-order reaction involving e<sub>CB</sub>-...EO<sup>+</sup> pairs associated with the same TiO<sub>2</sub> particle could be clearly discerned from charge recombination via bulk diffusion, and rate constants for these elementary steps have been derived. The encouraging result is that the intraparticle back-electron transfer is ca. 104 times slower than the forward injection. As a consequence, light-induced charge separation can be sustained in the semiconductor particle for at least several microseconds, which is sufficiently long to trap the injected electron by a noble metal deposited on its surface. These results should be important for the understanding of photosensitized electron transfer and photocatalysis which are widely used in photography and artificial photosynthesis.

Acknowledgment. Support of this work by the Schweizerische Nationalfonds zur Förderung der Wissenschaften and CIBA-GEIGY AG, Basel, is gratefully acknowledged. We are grateful to Dr. R. Humphry-Baker for assistance in the light-scattering experiments for particle size determination and to Dr. T. Geiger for performing cyclic voltammetric measurements to obtain the redox potential of eosin in water.

**Registry No.** TiO<sub>2</sub>, 13463-67-7; Eosin, 17372-87-1.

<sup>(47)</sup> Wilson, R. G. J. Appl. Phys. 1966, 37, 2261

<sup>(48)</sup> Tomkiewicz, M.; Huang, Y. S.; Pollak, F. J. Electrochem. Soc. 1983, 130, 1514.

<sup>(49)</sup> Mavroides, J. G.; Tchernev, D. I.; Kafulas, J. A.; Kolesar, D. F. Mater. Res. Bull. 1975, 10, 1023.

<sup>(50)</sup> Hope, G. A.; Bard, A. J. J. Phys. Chem. 1983, 87, 1979.

<sup>(51)</sup> Aspnes, D. E.; Heller, A. J. Phys. Chem. 1983, 87, 4919.

<sup>(52)</sup> Preliminary experiments show that addition of  $H_2$  does not change the features of the EO<sup>+</sup> decay in Figure 12a, indicating that  $k_{\text{trap}}$  is not affected by  $H_2$ . However, hydrogen was used also in the preparation of  $Pt/TiO_2$ , and this may have an effect on the type of junction formed.